THE JOURNAL OF BIOLOGICAL CHEMISTRY VOL. 285, NO. 33, pp. 25677–25685, August 13, 2010
Printed in the U.S.A.

Up-regulation of the Homophilic Adhesion Molecule Sidekick-1 in Podocytes Contributes to Glomerulosclerosis*

Received for publication, April 14, 2010, and in revised form, June 2, 2010 Published, JBC Papers in Press, June 18, 2010, DOI 10.1074/jbc.M110.133959

Lewis Kaufman[‡§1], Uma Potla[‡], Sarah Coleman[‡], Stanislav Dikiy[‡], Yutaka Hata[¶], Hidetake Kurihara[‖], John C. He[‡§], Vivette D. D'Agati[**], and Paul E. Klotman[‡]

*From the [‡]Division of Nephrology, Mount Sinai School of Medicine, New York, New York 10029, the [§]Division of Nephrology, James J. Peters Veterans Affairs Medical Center, Bronx, New York 10468, the [¶]Department of Medical Biochemistry, Graduate School of Medicine, Tokyo Medical and Dental University, Tokyo 113-8519, Japan, the [‖]Department of Anatomy, Juntendo University School of Medicine, Tokyo 113-8421, Japan, and the **Department of Pathology, Columbia University College of Physicians and Surgeons, New York, New York 10032*

Focal segmental glomerulosclerosis (FSGS) is a leading cause of nephrotic syndrome and end-stage renal disease worldwide. Although the mechanisms underlying this important disease are poorly understood, the glomerular podocyte clearly plays a central role in disease pathogenesis. In the current work, we demonstrate that the homophilic adhesion molecule sidekick-1 (*sdk-1*) is up-regulated in podocytes in FSGS both in rodent models and in human kidney biopsy samples. Transgenic mice that have podocyte-specific overexpression of *sdk-1* develop gradually progressive heavy proteinuria and severe FSGS. We also show that *sdk-1* associates with the slit diaphragm linker protein MAGI-1, which is already known to interact with several critical podocyte proteins including synaptopodin, α-actinin-4, nephrin, JAM4, and β-catenin. This interaction is mediated through a direct interaction between the carboxyl terminus of *sdk-1* and specific PDZ domains of MAGI-1. *In vitro* expression of *sdk-1* enables a dramatic recruitment of MAGI-1 to the cell membrane. Furthermore, a truncated version of *sdk-1* that is unable to bind to MAGI-1 does not induce podocyte dysfunction when overexpressed. We conclude that the up-regulation of *sdk-1* in podocytes is an important pathogenic factor in FSGS and that the mechanism involves disruption of the actin cytoskeleton possibly via alterations in MAGI-1 function.

Focal segmental glomerulosclerosis (FSGS)[2] is an important cause of end-stage renal disease worldwide, accounting for ~20% of all dialysis patients (1). In fact, the frequency of this disease has dramatically increased over the last 20 years, making it the most common cause of primary nephrotic syndrome in adults (1). Multiple cohort studies show progression to end-stage renal disease in 50–70% of cases at 10 years, giving FSGS one of the worst prognoses among primary glomerular diseases (2, 3).

The diagnosis of FSGS is based on the clinical findings of proteinuria and specific histopathological changes that include glomerular sclerosis, glomerular tuft collapse, and synechia formation. In the early stages, these changes are both focal, affecting a subset of glomeruli, and segmental, involving a portion of the glomerular tuft. Although the idiopathic form of FSGS is the most common, secondary FSGS occurs in association with other underlying conditions including HIV-associated nephropathy (HIVAN), among others.

Although the pathogenic mechanisms underlying this disease are poorly understood, the podocyte, the visceral epithelial cell of the glomerulus, plays a central role. Multiple genetic studies using both human and murine models demonstrate that the development of FSGS is initiated by podocyte dysfunction (4). In humans, mutations in the podocyte-specific genes nephrin (5), podocin (6), α-actinin-4 (7), TRPC6 (8, 9), and others all disrupt podocyte function, leading to inherited forms of FSGS. Two recent landmark studies showed a strong association of non-coding variants in the podocyte-expressed gene *myh9* with susceptibility to HIVAN and FSGS (10, 11), suggesting an important connection with the genetic predisposition of African-Americans to developing nephropathy and confirming the central role of podocyte genetics to many forms of renal failure.

Sidekick was first described in *Drosophila melanogaster* as a critical determinant of cell fate in retinal photoreceptors (12). Later, sidekick-1 (*sdk-1*) and its ortholog sidekick-2 (*sdk-2*) were found to localize to the neurological synapse and to function as guidance molecules targeting synapses to specific layers (13, 14). *sdk-1* and *sdk-2* each consist of a large extracellular domain containing six Ig motifs followed by 13 fibronectin type III repeats, a single transmembrane domain, and a short cytoplasmic tail containing a highly conserved PDZ binding domain at its carboxyl terminus. *sdk-1* and *sdk-2* function as homophilic adhesion molecules such that cells expressing *sdk-1* or *sdk-2* strongly prefer to interact exclusively with cells expressing the same sidekick isoform (13, 15).

We identified *sdk-1* as being massively overexpressed in podocytes in HIVAN (16, 17) and reported that this up-regulation was a maladaptive response resulting in increased intercellular adhesion and loss of cytoskeletal integrity (17). In the current work, we first demonstrate that *sdk-1* up-regulation in podocytes also occurs in idiopathic FSGS. We then validate the physiological relevance of this up-regulation by generating

* This work was supported, in whole or in part, by National Institutes of Health Grants K08 DK070530 (to L. K.) R01 DK084006 (to L. K.) and P01 DK056492 (to P. E. K.).

[1] To whom correspondence should be addressed: Division of Nephrology, Mount Sinai School of Medicine, One Gustave L. Levy Place, Box 1243, New York, NY 10029. Tel.: 212-241-6271; Fax: 212-987-0389; E-mail: lewis.kaufman@mssm.edu.

[2] The abbreviations used are: FSGS, focal segmental glomerulosclerosis; HIV, human immunodeficiency virus; HIVAN, HIV-associated nephropathy; MAGI, MAGUK with inverted domain structure; PAN, puromycin aminonucleoside; GST, glutathione *S*-transferase; MAGUK, membrane-associated guanylate kinase.

novel transgenic mice that develop severe FSGS when *sdk-1* is expressed specifically in podocytes. Next, we begin to dissect the mechanisms by which *sdk-1* up-regulation contributes to disease. We show that *sdk-1* directly interacts with the podocyte linker protein MAGI-1 and that this interaction is necessary for *sdk-1* overexpression to induce podocyte dysfunction. MAGUK with inverted domain structure-1 (MAGI-1) is localized specifically at the slit diaphragm in podocytes and is composed of one guanylate kinase, two WW domains, and six PDZ domains (18, 19). MAGI-1 is a linker protein that directly interacts with other critical podocyte proteins including α-actinin-4, synaptopodin, nephrin, JAM4, and β-catenin and is linked to the actin cytoskeleton through these proteins (20–23). We conclude that the up-regulation of *sdk-1* in podocytes is an important pathogenic factor in the development of FSGS and that the mechanism involves alterations in the actin cytoskeleton possibly mediated by changes in MAGI-1 scaffolding.

EXPERIMENTAL PROCEDURES

Human Kidney—Samples were collected under an approved institutional review board protocol from archived kidney biopsies at Columbia Presbyterian Medical Center. Cases with confirmed FSGS were used for analysis.

Murine Podocyte Cell Lines—Conditionally immortalized mouse podocytes were propagated and differentiated as described previously (41). Puromycin aminonucleoside (PAN) (Sigma-Aldrich) was added to the medium of differentiated podocytes at a concentration of 100 μg/ml for 48 h prior to RNA and protein extraction.

Quantitative PCR—Quantitative PCR was done using SYBR Green kit (Qiagen) per the manufacturer's protocol. Two sets of primers each spanning different introns were used, and the results were averaged. The primer pairs were: i) 5′-

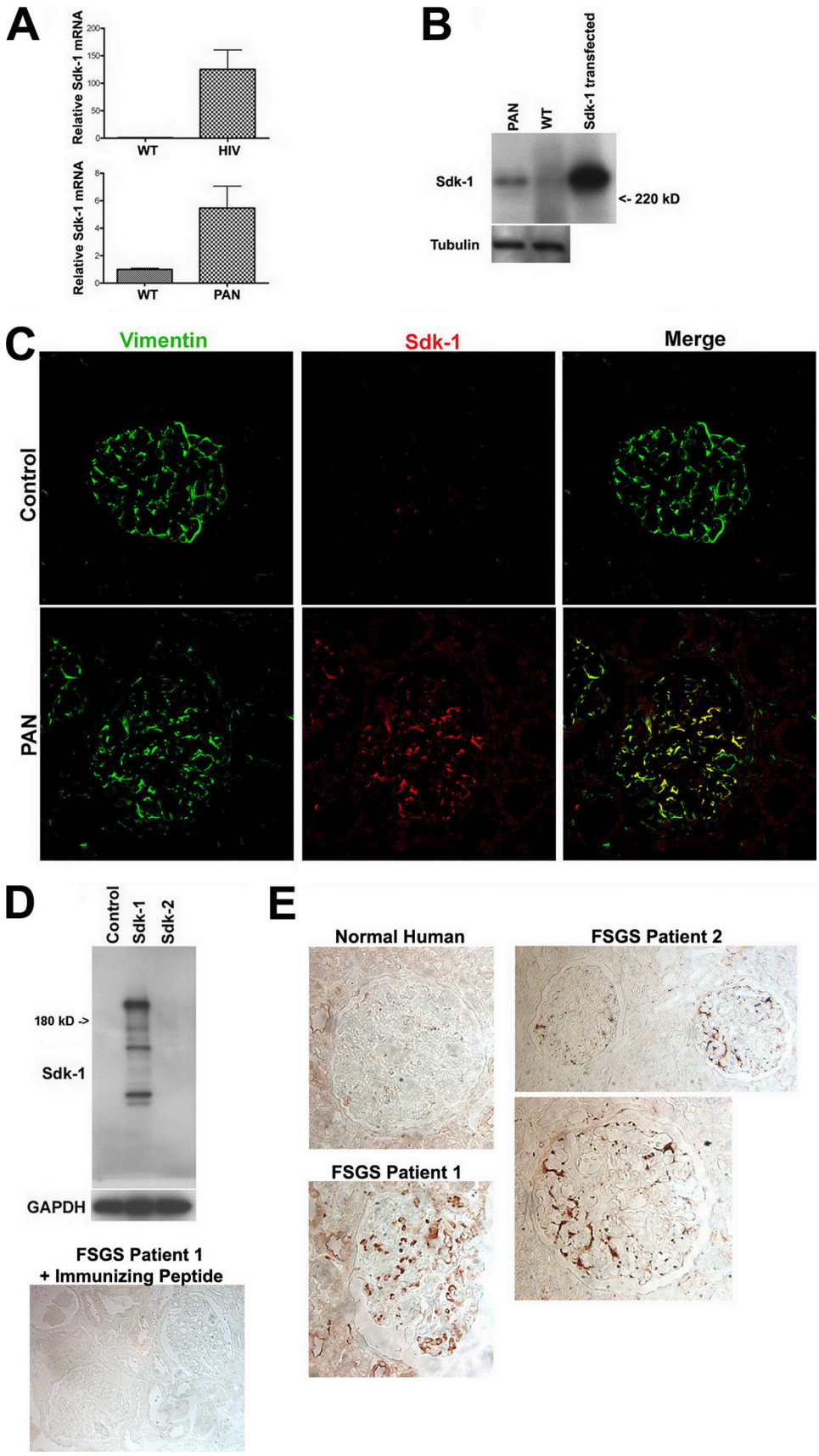

TCAAGGAGAAGTCGGTGGAT-3′ and 5′-GCCGCTTC-CAAGAGTTGTAG-3′ and ii) 5′-AACGGTCTTCTGCAAG-GCTA-3′ and 5′-TGTTCACGGTCTTGAAGCTG-3′.

Transgenic Animals—Full-length *sdk-1* cDNA was cloned into the vector pCCALL2-IRES-EGFP (gift of Dr. Susan Quaggin) and then linearized with Sca-I. The Mount Sinai Mouse Genetics Core Facility performed pronuclear injections to generate three FVB/N founders, two of which passed the transgene to subsequent progeny. Each line was bred to FVB/N podocin-Cre transgenic mice to generate double transgenic mice. The cre transgene was detected by PCR using the primers 5′-ATGTCCAATTTACTGACCG-3′ and 5′-CGCCGCATA-ACCAGTGAAC-3′. The PCCALL2 transgene was detected using primers that amplify a 500-bp portion of green fluorescent protein: 5′-AAGCTGACCCTGAAGTTCATCTG-3′ and 5′-AACTCCAGCAGGACCATGTGATC-3′. Histological analysis was done using formalin-fixed paraffin-embedded sections stained with periodic acid-Schiff. We performed electron microscopy on glutaraldehyde-fixed, epoxy-embedded tissue samples (JEOL 1010 electron microscope). Albuminuria was measured monthly using urine dipsticks. Mice were considered proteinuric for a dipstick reading of 2+ or greater that persisted for 2 consecutive months or if a mouse spontaneously expired after a single positive reading. Urine albumin and creatinine were measured in the chemistry laboratories of Mount Sinai Hospital via the Roche Diagnostics U/CSF protein (end point assay) method and the automated Jaffe method, respectively.

Antibodies and Immunostaining—Peptide antibodies directed to the human *sdk-1* C-terminal epitope GPGARTPLT-GFSSFV were produced in rabbit (Open Biosystems). This epitope differs from the murine version by a single peptide. Specificity of the antiserum was confirmed by Western blotting on lysates of 293T cells transfected (Effectene, Qiagen) with mouse *sdk-1* or *sdk-2* expression plasmids. Specificity was confirmed by doing immunostaining after preincubating the antiserum with excess immunizing peptide (0.5 mg/ml). Other primary antibodies used include: *sdk-1* (antibody number 3534) as described previously (17), Ki-67 (Vector Laboratories), and synaptopodin (gift of Dr. Peter Mundel). PAN nephrosis in rats was induced, and immunofluorescence was done on frozen sections as described previously (22).

Immunoprecipitation—FLAG-*sdk1* and FLAG-*sdk-1*-C-del expression plasmids were generated by PCR amplifying the intracellular (including the transmembrane domain) portion of *sdk-1* and then subcloning the products into pFLAG-CMV-2 (Sigma-Aldrich). For FLAG-*sdk-1*-C-del, a stop codon was added to the antisense primer. The sense primer for both constructs was 5′-ACGAATTCAGTGTCAGCACAAGCT-GAAGCC-3′, the antisense primer for FLAG-*sdk-1* was 5′-GAGGATCCATGTCACACGAAGGAGGAGAA-3′, and the antisense primer for FLAG-*sdk-1*-C-del was 5′-GAGGATC-CTCAGCCAGCTGGTGTGTAGACTCCGCC-3′. PCR products and pFLAG-CMV-2 were digested with BamHI and EcoRI and then ligated. Positive clones were confirmed by direct sequencing.

293T cells were transfected with either FLAG-*sdk1* or FLAG-*sdk-1*-C-del. Total protein lysates were incubated with anti-FLAG M2 agarose (Sigma-Aldrich). Agarose beads were washed and then incubated with differentiated podocyte lysate overnight. Bound proteins were analyzed by Western blotting using anti-MAGI-1 antibody (Sigma-Aldrich).

Myc-tagged MAGI-1 constructs were previously described (22). To do pull downs, 293T cells were transfected with each Myc-MAGI construct. Lysates were added to anti-FLAG M2 beads that had been bound to FLAG-*sdk1* or FLAG-*sdk-1*-C-del protein and then incubated overnight. Precipitates were analyzed by Western blot using rabbit anti-Myc antibody (Sigma-Aldrich).

GST-MAGI-1 (PDZ1, PDZ4, PDZ5) constructs were previously described (20). Bacterial transformants for each plasmid were generated in BL21 codon plus cells (Amersham Biosciences). After induction with 0.5 mM isopropyl-1-thio-β-D-galactopyranoside, bacterial lysates were incubated with glutathione-Sepharose beads. 293T cellular lysates containing either FLAG-*sdk-1* or FLAG-*sdk-1*-C-del proteins were added to the washed beads. The next day, bound proteins were released by boiling and then analyzed by Western blot using M2 anti-FLAG.

Glomerular isolation was performed using serial sieving of 180-, 106-, and 71-μm diameter. Glomerular lysates from 12 kidneys were collected and pooled for each group. To do immunoprecipitation, lysates were incubated with either anti-*sdk-1* (antibody number 3534) (17) or normal rabbit serum fixed on protein A-agarose. After washing, precipitates were analyzed by Western blotting for MAGI-1.

sdk-1 Expression Plasmids and Stable Podocyte Transfectants—An *sdk-1* expression plasmid that codes for a truncated *sdk-1* protein lacking its C-terminal four amino acids (ΔSSFV) was generated using a PCR-based protocol. The plasmid pcDNA3.1/*sdk-1* was digested with HpaI and DraI, and the 1.75-kb fragment was subcloned into the SmaI site of PGEM3Z. The mutagenic primers, 5′-CTACCCTGATGGAGGCGTGA-TGTCAGAAGCCGGTGAGGGGGGCCCGGGCT-3′ and 5′-AGCCCGGGCCCCCCTCACCGGCTTCTGACATCACGC-CTCCATCAGGGTAG-3′, were used to amplify the entire plasmid followed by digestion of template DNA with Dpn1. After transformation, positive clones were confirmed to carry the desired mutation by direct sequencing. The mutagenic

FIGURE 1. ***sdk-1* is overexpressed in podocytes in FSGS.** *A*, expression of *sdk-1* RNA is significantly up-regulated in podocytes in cell culture when exposed to either HIV-1 infection or PAN as determined by quantitative PCR. Massive up-regulation of *sdk-1* RNA after HIV-1 infection was previously reported (16, 17). *WT*, wild type. *Error bars* indicate S.E. *B*, the up-regulation of *sdk-1* protein after exposure to PAN was confirmed by Western blotting. *C*, 293T cells transfected with an *sdk*-1 expression construct were used as the positive control. *C*, *sdk-1* protein expression was detected by immunofluorescence in podocytes in PAN-treated rats but not in sham-injected controls. Podocyte-specific expression was confirmed by colocalization with the podocyte-specific marker vimentin. *D*, *upper*, a novel rabbit anti-human *sdk-1* antibody specifically interacts with lysate from cells transfected with an *sdk-1*, but not an *sdk-2*, expression plasmid. *Lower*, when preincubated with excess immunizing peptide, this antibody showed no reactivity against human specimens. *GAPDH*, glyceraldehyde-3-phosphate dehydrogenase. *E*, by immunohistochemistry, *sdk-1* protein was detected in a podocyte distribution in kidney biopsies from two patients with idiopathic FSGS but not in normal human kidney.

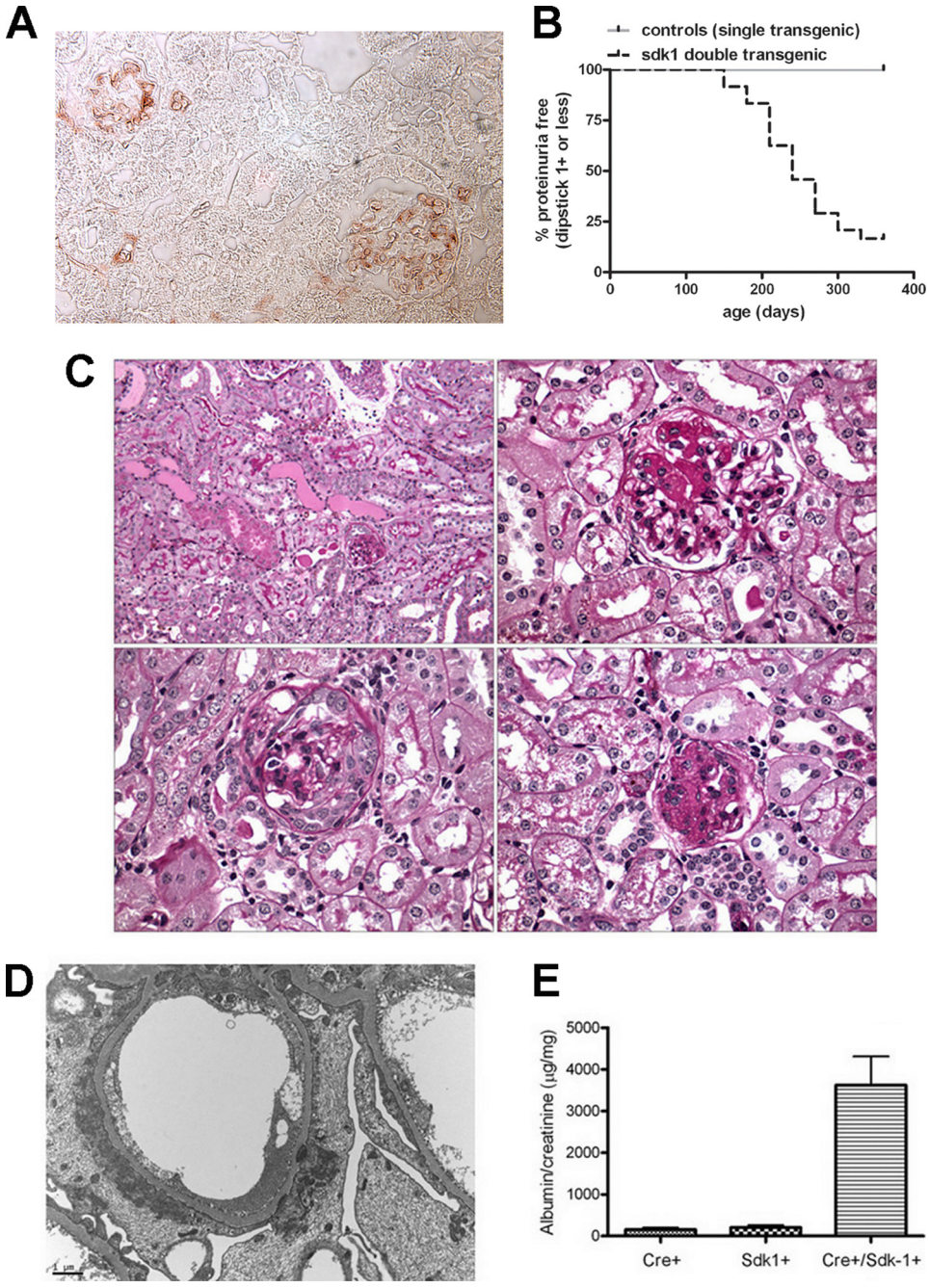

FIGURE 2. **De novo expression of *sdk-1* specifically in podocytes *in vivo* leads to FSGS.** *A*, double transgenic mice (carrying both podocin-Cre and floxed *sdk-1* transgenes) express *sdk-1* specifically in podocytes as determined by immunostaining. *B*, monthly urine dipstick measurements were recorded for double transgenic ($n = 22$), podocin-Cre alone ($n = 5$) and floxed *sdk-1* alone ($n = 5$) mice for a total of 1 year. Double transgenic mice begin to develop overt proteinuria at an age of 5 months as compared with single transgenic littermates that did not become proteinuric. Mice were considered proteinuric for a dipstick reading of 2+ or greater that persisted for 2 consecutive months or if an animal expired spontaneously after a single positive reading before a second reading could be performed. *C*, at 9 months of age, double transgenic mice were sacrificed, and kidneys were harvested for routine pathology . Periodic acid-Schiff staining demonstrates protein casts and tubular protein resorption droplets (*upper left*, 20×), classic FSGS lesions (*upper right*, 60×), glomerulus with collapse and epithelial cell proliferation with pseudocrescent (*lower left*), and a globally sclerotic glomerulus (*lower right*). *D*, electron microscopy shows severe foot process effacement with condensation of actin filaments above the glomerular basement membrane, and focal cytoplasmic vacuolization. *E*, urine albumin:creatinine ratios shows massive proteinuria in double transgenic animals as compared with single transgenic littermates. *Error bars* indicate S.E.

sequence was excised from the PGEM3Z vector and subcloned in frame into pIRES-*sdk-1*-GFP.

To generate stable podocyte transfectants, each expression vector was introduced into undifferentiated podocytes using Amaxa Nucleofection kit. Cells were then propagated in medium containing 400 ng/μl Geneticin. Prior to experiments, cells were differentiated at 37 °C on collagen-coated coverslips. Phalloidin staining was done using Alexa Fluor phalloidin-594 according to the manufacturer's instructions (Molecular Probes).

Quantification of Stress Fibers—Two blinded observers counted 200 cells/sample from randomly chosen fields for the presence of clearly defined, non-centrifugal, stress fibers. The percentage of stress fiber positive cells was calculated for each observer and then averaged.

Statistical Analysis—Student's paired *t* test was used to analyze the difference between the groups. Results were considered significant at p values < 0.05.

RESULTS

sdk-1 Is Overexpressed in Podocytes in FSGS—In cultured podocytes, either expression of HIV-1 genes or exposure to PAN, two widely used models of podocyte injury and FSGS, induced significant up-regulation of *sdk-1* mRNA expression as determined by quantitative PCR (Fig. 1*A*). The up-regulation of *sdk-1* in HIV-1 podocytes has been confirmed previously (16, 17). Western blotting confirmed the up-regulation of *sdk-1* protein in the setting of PAN exposure in culture (Fig. 1*B*). To validate our findings in animals, we performed double immunofluorescent staining for *sdk-1* and the podocyte-specific protein vimentin, comparing kidneys from control-injected with PAN-injected rats. Our data showed up-regulation of *sdk-1* specifically in podocytes in PAN nephrosis (Fig. 1*C*).

To evaluate the relevance to human FSGS, we performed immunohistochemistry for *sdk-1* on three human kidney biopsy samples with confirmed idiopathic FSGS. A rabbit anti-human *sdk-1* antibody was generated and found to specifically recognize *sdk-1* on Western blotting (Fig. 1*D*). Preincubating the antiserum with excess immunizing peptide eliminated all reactivity on immunohistochemistry (Fig. 1*D*).

Using this antibody, *sdk-1* expression was detected in a podocyte-like distribution in two of the three idiopathic FSGS biopsies but was almost completely absent in normal human kidney controls (Fig. 1*E*). Interestingly, staining was present in non-sclerotic as well as in some sclerotic glomeruli, suggesting that *sdk-1* up-regulation may occur prior to the development of overt glomerulosclerosis.

Targeted Overexpression of sdk-1 in Podocytes in Transgenic Mice Results in FSGS—To determine the *in vivo* consequences of *sdk-1* up-regulation, we generated novel transgenic mice that overexpress *sdk-1* specifically in podocytes. The transgene contains lox-P sites flanking spacer DNA, which separates the β-actin promoter from *sdk-1*. In the presence of cre recombinase, the spacer DNA is removed, bringing *sdk-1* near a strong promoter. We bred our floxed mice to mice bearing a transgene containing cre recombinase under the podocyte-specific podocin promoter. These double transgenic animals demonstrate strong expression of *sdk-1* specifically in glomeruli in a clear podocyte distribution (Fig. 2*A*), whereas single transgenic littermates showed little if any *sdk-1* expression (not shown).

Most double transgenic mice develop massive proteinuria at between 5 and 10 months of age (Fig. 2*B*) as compared with single transgenic littermates that did not develop proteinuria. Pathology shows FSGS with 5–50% of glomeruli affected (Fig. 2*C*). This phenotype is similar in each of two founding lines, verifying that the phenotype is unrelated to the chromosomal location of transgene insertion. The majority of affected glomeruli showed classic FSGS lesions with apparent podocyte loss and synechia formation (Fig. 2*C*, *upper right*). A smaller number of glomeruli showed podocyte hypertrophy surrounding areas of scar with evidence of glomerular epithelial cell proliferation and pseudocrescent formation (Fig. 2*C*, *lower left*), a phenotype highly reminiscent of collapsing FSGS including HIVAN. Electron microscopy showed severe foot process effacement and condensation of actin filaments forming a cytoskeletal mat above the glomerular basement membrane, as well as focal intracytoplasmic vacuoles and transport vesicles (Fig. 2*D*). Urine albumin:creatinine ratios confirmed massive proteinuria in double transgenic animals as compared with single transgenic littermates at 9 months of age (Fig. 2*E*). Mice did not develop renal failure as determined by measurement of blood urea nitrogen and creatinine concentrations but did demonstrate a reduced survival after the onset of nephrotic range proteinuria, with most affected animals dying by 14 months of age.

Expression of the podocyte differentiation marker synaptopodin was lost in areas of scar within affected glomeruli (Fig. 3*A*). This focal loss is most consistent with idiopathic FSGS, whereas collapsing FSGS would typically show global loss of synaptopodin within an affected glomerulus (24). Interestingly, Ki-67 was strongly expressed both within proliferating glomerular epithelial cells making up a pseudocrescent and in podocytes within the glomerular tuft (Fig. 3*B*). These features combine characteristics of FSGS (focal loss of synaptopodin) with those of collapsing glomerulopathy (increased epithelial cell proliferation).

sdk-1 Interacts with the Slit Diaphragm Protein MAGI-1—*sdk-1* and *sdk-2* contain highly conserved PDZ binding

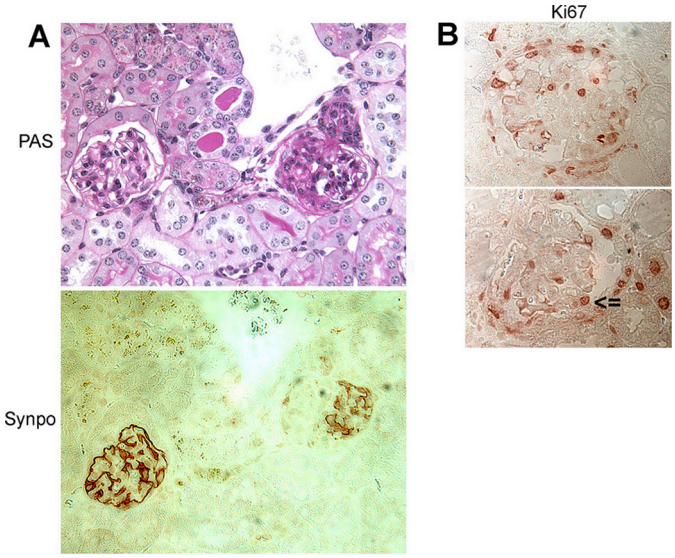

FIGURE 3. **Podocyte-specific expression of *sdk-1* in transgenic mice induces FSGS that has elements of both idiopathic and collapsing types.** *A*, synaptopodin (*Synpo*) expression is focally lost in sclerotic glomeruli but is preserved in unaffected areas. *PAS*, periodic acid-Schiff. *B*, high levels of Ki-67 expression were seen in cells making up a pseudocrescent (*upper panel*) and in podocytes within the glomerular tuft (*lower panel*; *arrowhead* identifies a podocyte).

domains at their carboxyl termini. Previously, yeast two-hybrid screening identified MAGI-1 as a potential ligand for *sdk-2* (25). Because *sdk-1* and *sdk-2* contain identical PDZ binding domains, we anticipated that they would have similar binding specificities.

To confirm an interaction between *sdk-1* and MAGI-1, we generated expression constructs for both FLAG-tagged *sdk-1* and a truncated FLAG-tagged *sdk-1* (FLAG-*sdk-1*-C-del) that lacks its 14 carboxyl-terminal amino acids. We used these FLAG-tagged proteins as bait to do pull downs from podocyte cellular lysate (Fig. 4*A*). The three splice variants of MAGI-1 all interact with full-length *sdk-1*, but none interact with the truncated version. This implies a specific interaction between *sdk-1* and at least one of the PDZ domains of MAGI-1.

To confirm this interaction *in vivo*, we extracted glomerular lysates from proteinuric *sdk-1* double transgenic mice and from age-matched controls using successive glomerular sieving. We precipitated MAGI-1 from double transgenic glomerular lysate using an anti-*sdk-1* antibody as bait but not when using control IgG as bait (Fig. 4*B*). MAGI-1 could not be precipitated from wild-type glomerular lysate when using either anti-*sdk-1* antibodies or control IgG as bait. These experiments suggest an *in vivo* interaction between *sdk-1* and MAGI-1 in our FSGS mouse model.

To determine whether expression of *sdk-1* could alter the localization of MAGI-1 protein, we performed cotransfection experiments in HEK293T cells (Fig. 4*C*). When Myc-MAGI-1 was expressed alone, it appeared exclusively in the cytoplasm (26). However, in cells expressing both Myc-MAGI-1 and full-length *sdk-1*, there was a dramatic recruitment of Myc-MAGI-1 to the membrane where the two proteins colocalized especially at sites of intercellular contact. We also generated an *sdk-1* expression vector that produces a truncated version of *sdk-1* that lacks its last four amino acids (ΔSSFV). When ΔSSFV

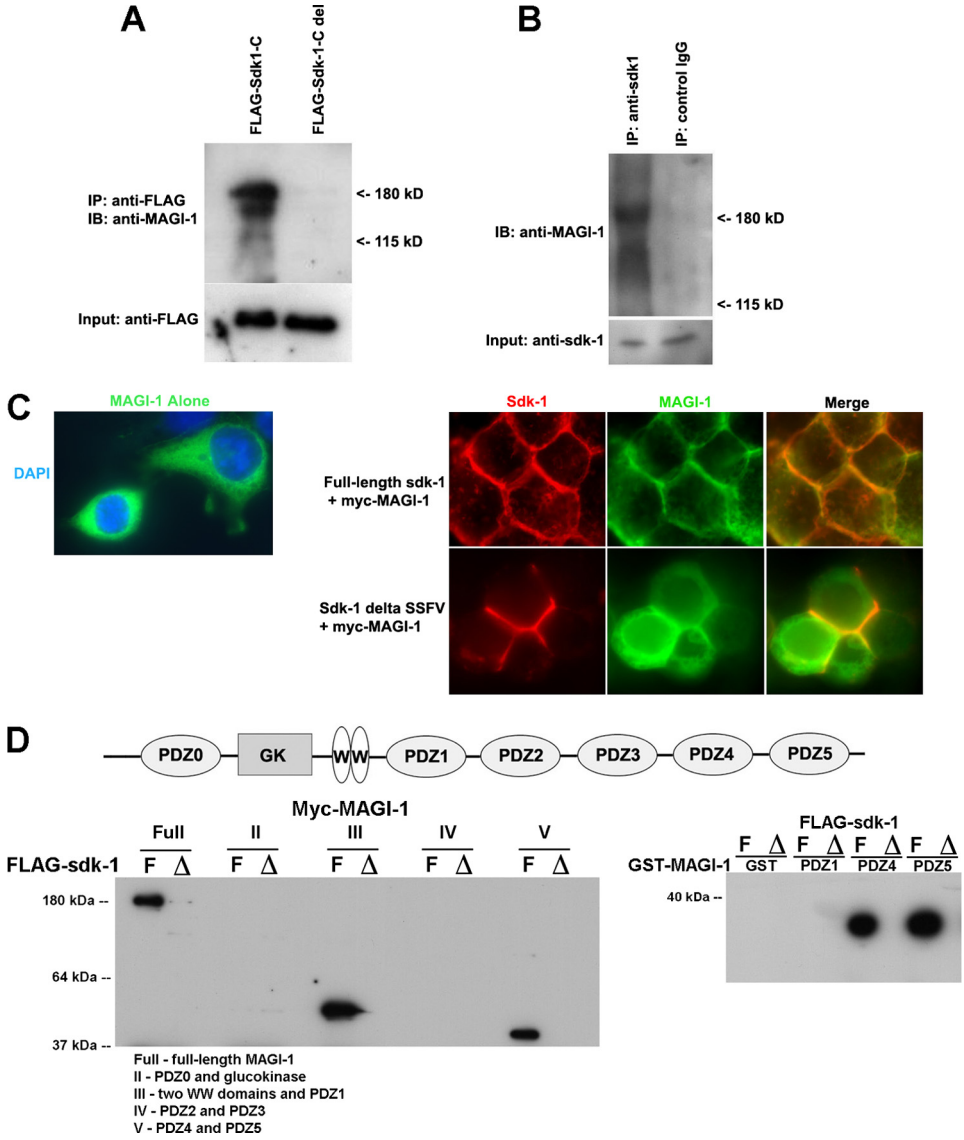

FIGURE 4. **MAGI-1 directly interacts with *sdk-1*.** *A*, all splice variants of MAGI-1 were precipitated from podocyte cellular lysate using a full-length FLAG-*sdk-1* protein as bait, but not with a truncated version that lacks its PDZ binding domain. *IP*, immunoprecipitation; *IB*, immunoblotting. *B*, MAGI-1 was endogenously precipitated from double transgenic mouse glomerular protein lysate using an anti-*sdk-1* antibody but not when using control IgG. *C*, Myc-MAGI localizes to the cytoplasm of transfected 293T cells when expressed alone (*left*). However, when Myc-MAGI-1 is co-expressed with full-length *sdk-1*, there is a dramatic recruitment of MAGI-I protein to the membrane, where it colocalizes with *sdk-1* particularly at sites of intercellular contact. However, when Myc-MAGI-1 and a truncated *sdk-1* that lacks its PDZ binding domain are co-expressed, Myc-MAG-I remains primarily cytoplasmic (with clear exclusion of the nuclear compartment), whereas *sdk-1* is still in the membrane. *DAPI*, 4′,6-diamidino-2-phenylindole. *D*, various Myc-tagged MAGI proteins were expressed in 293T cells. *Full* contains all domains of MAGI including all six PDZ domains (schematic shown in *top panel*); *II* contains PDZ0 and glucokinase (*GK*); *III* contains two WW domains and PDZ1; *IV* contains PDZ2 and PDZ3; and *V* contains PDZ4 and PDZ5 (described in Ref. 22). Lysates were incubated with FLAG beads that had been bound to either FLAG-*sdk-1*-Full (*F*) or FLAG-*sdk-1*-Delete (Δ) that lacks its C terminus, and pulldowns were performed with Western blotting for Myc (*lower left*). GST fusion proteins encoding individual PDZ domains of MAGI-1 (PDZ1, PDZ4, and PDZ5 (described in Ref. 20)) were expressed in bacteria, and lysates were bound to glutathione-Sepharose beads. Lysates containing FLAG-*sdk-1*-Full and FLAG-*sdk-1*-Delete proteins were added to the beads, and pulldown assays were performed with Western blotting for FLAG (*lower right*). These results suggest that *sdk-1* binds to PDZ1, PDZ4, and PDZ5 of MAGI-1 but that, unlike for PDZ4 and PDZ5, PDZ1 as a single domain is not sufficient to mediate the interaction.

was expressed with Myc-MAGI-1 in 293T cells, MAGI-1 remained cytoplasmic with clear exclusion of the nuclear compartment, whereas the localization of *sdk-1* did not change significantly. Overall, this supports the specificity of the interaction between *sdk-1* and MAGI-1 and suggests that *sdk-1* expression can alter the cellular localization of MAGI-1.

sdk-1 Binds to PDZ1, PDZ4, and PDZ5 of MAGI-1—To identify the specific domain of MAGI-1 responsible for *sdk-1* binding, we used FLAG-*sdk-1* and *FLAG-sdk-1*-C-del as bait to pull down various Myc-tagged MAGI-1 constructs that were previously described (22). The Myc-tagged MAGI-1 constructs were as follows. *Full* contained full-length MAGI-1 including all six PDZ domains (schematic shown in Fig. 4*D*, *top*), *II* carried PDZ0 and the glucokinase domain, *III* carried the two WW domains and PDZ1, *IV* contained PDZ2 and PDZ3, and *V* carried PDZ4 and PDZ5. Full-length Myc-MAGI-1, Myc-MAGI-1 III, and Myc-MAGI-1 V were precipitated by FLAG-*sdk-1* full, implying that PDZ0, PDZ2, and PDZ3 were not responsible for the interaction with *sdk-1* (Fig. 4*D*, *lower left*).

To further define the responsible domains, we performed pulldown assays using GST fusion proteins containing the implicated individual PDZ domains of MAGI-1 (PDZ1, PDZ4, PDZ5) (20). Lysates of 293T cells expressing either FLAG-*sdk-1* or FLAG-*sdk-1*-C-del were incubated with individual GST-MAGI-1 constructs that were immobilized on glutathione-Sepharose beads. MAGI-1 PDZ4, and PDZ5 but not PDZ1 or GST alone, interacted with FLAG-*sdk-1* (Fig. 4*D*, *lower right*). None of them interacted with FLAG-*sdk-1*-C-del. The fact that PDZ1 did not bind to *sdk-1* in the GST pulldown assay suggests that the sequence upstream of PDZ1, possibly including all or part of the WW domains, is required for binding.

A Truncated Version of sdk-1 That Is Unable to Bind to MAGI-1 Does Not Induce Podocyte Dysfunction—Previously, we reported that podocytes stably transfected with a full-length *sdk-1* expression construct displayed a simplified cell shape and loss of normal actin cytoskeletal structure characterized by a centrifugal distribution of actin filaments (17). To identify the relevance of the interaction between *sdk-1* and MAGI-1, we generated a stably transfected podocyte cell line that expresses a truncated version of *sdk-1* that lacks its PDZ binding domain and is unable to bind

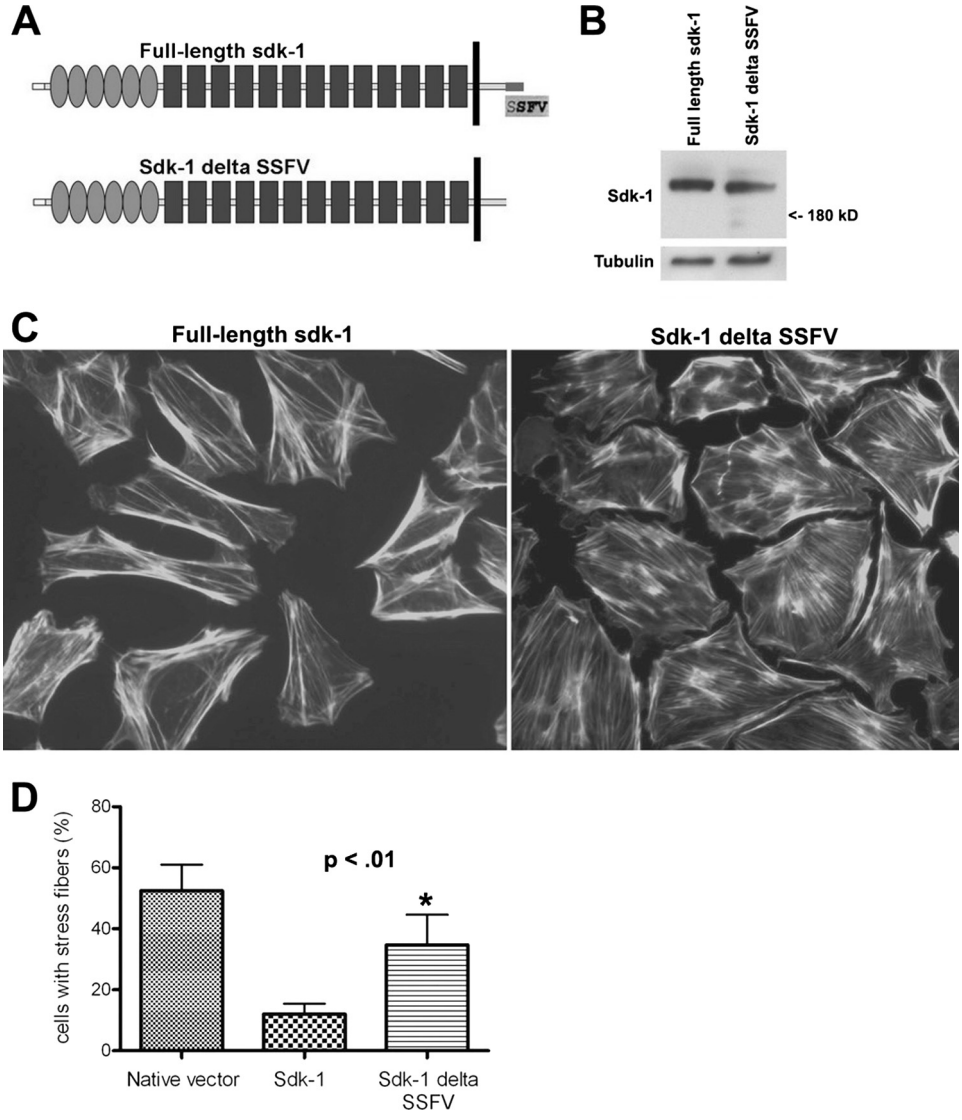

FIGURE 5. **A truncated version of *sdk-1* that is unable to bind to MAGI-1 does not induce podocyte dysfunction when overexpressed.** *A*, as shown in the schematic representation, *sdk-1* ΔSSFV is identical to full-length *sdk-1* except for a deletion of its last four amino acids. *B*, podocyte cell lines stably transfected with full-length *sdk-1* or the truncated version express similar levels of *sdk-1* protein. *C*, podocytes stably transfected with the full-length *sdk-1* expression plasmid show dramatic loss of normal actin cytoskeletal structure characterized by a centrifugal distribution of actin filaments as determined by phalloidin staining as compared with podocytes expressing *sdk-1* ΔSSFV. *D*, two blinded observers each counted from random fields the number of cells containing substantial stress fibers throughout the entire cell (in a non-centrifugal distribution). The percentage of positive cells was calculated per observer and then averaged (*, $p < 0.01$). *Error bars* indicate S.E.

to MAGI-1 (ΔSSFV, Fig. 5*A*). Although both podocyte cell lines showed similar levels of *sdk-1* expression (Fig. 5*B*), podocytes expressing truncated *sdk-1* protein were dramatically better able to form normal stress fibers throughout the entire cell (in a non-centrifugal pattern) as compared with podocytes expressing the full-length version (Fig. 5, *C* and *D*). This implies that the ability of *sdk-1* to induce podocyte dysfunction is dependent on its ability to interact with cytoplasmic scaffolding molecules such as MAGI-1.

DISCUSSION

In the current work, we have identified a novel mouse model of chronic FSGS mediated by a unique cellular mechanism that is relevant to human disease. *De novo* expression of *sdk-1* in podocytes was sufficient to induce slowly progressive glomerulosclerosis in transgenic mice. Affected animals develop relatively late onset proteinuria, without renal failure, that does not begin until well into adulthood and then progresses over many months. This is in stark contrast to existing models of FSGS that typically involve early onset proteinuria with rapid progression to kidney failure and death. These rapidly progressive FSGS models include knock-out models (CD2AP (27), neph1 (28), α-actinin-4 (29), podocin (30), nephrin (31), and others) and podocyte-specific overexpression models such as Notch-1 (32, 33). Overexpression of *sdk-1* in podocytes also induced changes that are typical for the collapsing variant of FSGS including podocyte hyperplasia, hypertrophy, pseudocrescent formation, and expression of the cell cycle marker Ki-67. Several other mouse models of collapsing glomerulopathy have been described including: α-actinin-4 knock-in and knock-out models (34), transgenic mice with podocyte-specific overexpression of vascular endothelial growth factor (35), alterations in mitochondrial function (36), and expression of HIV genes (37). Again, these other FSGS models are characterized by relatively rapid disease progression. The late onset and more gradual disease progression evident in the *sdk-1* transgenic model are more consistent with the usual clinical course of human FSGS patients. We propose our model to be one of the first genetic models of chronic, slowly progressive FSGS.

We do note significant differences in the relative amounts of observed glomerulosclerosis between animals and some differences in age of onset of proteinuria and rapidity of progression; this is likely explained by observed differences in expression levels of *sdk-1* both between animals and even in different glomeruli within a given animal. The reason for these differences is uncertain but seems to be related to variable expression of cre recombinase between glomeruli.

To investigate the mechanisms by which *sdk-1* up-regulation in the podocyte contributes to FSGS pathogenesis, we began to investigate how *sdk-1* interacts with other important podocyte proteins. The cytoplasmic domains of *sdk-1* and *sdk-2* contain no clear signaling domains other than a highly conserved car-

boxyl-terminal PDZ binding domain. In fact, the six terminal amino acids (GFSSFV) are completely conserved in all sidekicks in all available species from *Caenorhabditis elegans* to humans, suggesting that binding to this conserved domain is critical to sidekick function. In this way, we identified the slit diaphragm linker protein MAGI-1 as binding specifically to this conserved motif.

The MAGI proteins, with their multiple protein-protein interacting domains, have a large number of known binding partners. In podocytes, for example, MAGI-1 is known to interact with synaptopodin via its WW domain (21), with α-actinin-4 via PDZ domain 5 (21), with nephrin via PDZ domains 2 and 3 (22),with JAM4 via PDZ domains 1 and 4 (20), and with β-catenin via PDZ domain 5 (38). Presumably, MAGI-1 functions to stabilize and organize this complex of proteins at the slit diaphragm and to link them to the actin cytoskeleton. Because the phenotype of MAGI-1 null mice has not yet been reported, the importance of MAGI-1 as a stabilizing or signaling molecule in the podocyte has not been fully established. Furthermore, at this time, no human familial nephrotic syndrome cases have been linked to mutations in MAGI-1.

In this work, we show that the interaction between *sdk-1* and MAGI-1 is promiscuous in that three different PDZ domains of MAGI-1 are each capable of binding to the PDZ binding domain of *sdk-1*. Expression of *sdk-1* was also able to change the subcellular localization of MAGI-1 by inducing dramatic recruitment to the cell membrane. Furthermore, a truncated version of *sdk-1* that lacks its terminal four amino acids is unable to interact with MAGI-1 and does not induce podocyte dysfunction when overexpressed. These data imply, but do not definitively prove, that the interaction between the two proteins is important for induction of disease. It is possible that *sdk-1* interacts with other molecules besides MAGI-1 and that these other interactions are also important in inducing podocyte dysfunction. Ongoing work is focused on clarifying these possibilities.

The interaction between *sdk-1* and MAGI-1 may also be important to the process of neuronal synapse formation. In brain development, both proteins are highly expressed specifically at neurological synapses, and both affect the processes of synaptic connectivity and neuronal migration (13, 14, 26, 39, 40). *sdk-2* is also important in this process, and because its PDZ binding domain is identical to that of *sdk-1*, it is also likely to interact with MAGI-1, although this has not been shown.

Collectively, our data identify a novel mouse model of chronic FSGS that implicates the *sdk-1* genetic pathway as important to the pathogenesis of glomerular sclerosis. These findings suggest that the up-regulation of *sdk-1* by podocytes in FSGS is a maladaptive response to injury that is independently capable of leading to progressive podocyte dysfunction and ultimately to glomerular sclerosis.

REFERENCES

1. Kitiyakara, C., Eggers, P., and Kopp, J. B. (2004) *Am. J. Kidney Dis.* **44,** 815–825
2. Rydel, J. J., Korbet, S. M., Borok, R. Z., and Schwartz, M. M. (1995) *Am. J. Kidney Dis.* **25,** 534–542
3. Korbet, S. M., Schwartz, M. M., and Lewis, E. J. (1994) *Am. J. Kidney Dis.* **23,** 773–783
4. Pollak, M. R. (2003) *Semin. Nephrol.* **23,** 141–146
5. Kestilä, M., Lenkkeri, U., Männikkö, M., Lamerdin, J., McCready, P., Putaala, H., Ruotsalainen, V., Morita, T., Nissinen, M., Herva, R., Kashtan, C. E., Peltonen, L., Holmberg, C., Olsen, A., and Tryggvason, K. (1998) *Mol. Cell* **1,** 575–582
6. Boute, N., Gribouval, O., Roselli, S., Benessy, F., Lee, H., Fuchshuber, A., Dahan, K., Gubler, M. C., Niaudet, P., and Antignac, C. (2000) *Nat. Genet.* **24,** 349–354
7. Kaplan, J. M., Kim, S. H., North, K. N., Rennke, H., Correia, L. A., Tong, H. Q., Mathis, B. J., Rodríguez-Pérez, J. C., Allen, P. G., Beggs, A. H., and Pollak, M. R. (2000) *Nat. Genet.* **24,** 251–256
8. Winn, M. P., Conlon, P. J., Lynn, K. L., Farrington, M. K., Creazzo, T., Hawkins, A. F., Daskalakis, N., Kwan, S. Y., Ebersviller, S., Burchette, J. L., Pericak-Vance, M. A., Howell, D. N., Vance, J. M., and Rosenberg, P. B. (2005) *Science* **308,** 1801–1804
9. Reiser, J., Polu, K. R., Möller, C. C., Kenlan, P., Altintas, M. M., Wei, C., Faul, C., Herbert, S., Villegas, I., Avila-Casado, C., McGee, M., Sugimoto, H., Brown, D., Kalluri, R., Mundel, P., Smith, P. L., Clapham, D. E., and Pollak, M. R. (2005) *Nat. Genet.* **37,** 739–744
10. Kopp, J. B., Smith, M. W., Nelson, G. W., Johnson, R. C., Freedman, B. I., Bowden, D. W., Oleksyk, T., McKenzie, L. M., Kajiyama, H., Ahuja, T. S., Berns, J. S., Briggs, W., Cho, M. E., Dart, R. A., Kimmel, P. L., Korbet, S. M., Michel, D. M., Mokrzycki, M. H., Schelling, J. R., Simon, E., Trachtman, H., Vlahov, D., and Winkler, C. A. (2008) *Nat. Genet.* **40,** 1175–1184
11. Kao, W. H., Klag, M. J., Meoni, L. A., Reich, D., Berthier-Schaad, Y., Li, M., Coresh, J., Patterson, N., Tandon, A., Powe, N. R., Fink, N. E., Sadler, J. H., Weir, M. R., Abboud, H. E., Adler, S. G., Divers, J., Iyengar, S. K., Freedman, B. I., Kimmel, P. L., Knowler, W. C., Kohn, O. F., Kramp, K., Leehey, D. J., Nicholas, S. B., Pahl, M. V., Schelling, J. R., Sedor, J. R., Thornley-Brown, D., Winkler, C. A., Smith, M. W., and Parekh, R. S. (2008) *Nat. Genet.* **40,** 1185–1192
12. Nguyen, D. N., Liu, Y., Litsky, M. L., and Reinke, R. (1997) *Development* **124,** 3303–3312
13. Yamagata, M., Weiner, J. A., and Sanes, J. R. (2002) *Cell* **110,** 649–660
14. Yamagata, M., and Sanes, J. R. (2008) *Nature* **451,** 465–469
15. Hayashi, K., Kaufman, L., Ross, M. D., and Klotman, P. E. (2005) *FASEB J.* **19,** 614–616
16. Kaufman, L., Hayashi, K., Ross, M. J., Ross, M. D., and Klotman, P. E. (2004) *J. Am. Soc. Nephrol.* **15,** 1721–1730
17. Kaufman, L., Yang, G., Hayashi, K., Ashby, J. R., Huang, L., Ross, M. J., Klotman, M. E., and Klotman, P. E. (2007) *FASEB J.* **21,** 1367–1375
18. Dobrosotskaya, I., Guy, R. K., and James, G. L. (1997) *J. Biol. Chem.* **272,** 31589–31597
19. Ide, N., Hata, Y., Nishioka, H., Hirao, K., Yao, I., Deguchi, M., Mizoguchi, A., Nishimori, H., Tokino, T., Nakamura, Y., and Takai, Y. (1999) *Oncogene* **18,** 7810–7815
20. Hirabayashi, S., Tajima, M., Yao, I., Nishimura, W., Mori, H., and Hata, Y. (2003) *Mol. Cell. Biol.* **23,** 4267–4282
21. Patrie, K. M., Drescher, A. J., Welihinda, A., Mundel, P., and Margolis, B. (2002) *J. Biol. Chem.* **277,** 30183–30190
22. Hirabayashi, S., Mori, H., Kansaku, A., Kurihara, H., Sakai, T., Shimizu, F., Kawachi, H., and Hata, Y. (2005) *Lab. Invest.* **85,** 1528–1543
23. Sakurai, A., Fukuhara, S., Yamagishi, A., Sako, K., Kamioka, Y., Masuda, M., Nakaoka, Y., and Mochizuki, N. (2006) *Mol. Biol. Cell* **17,** 966–976
24. Barisoni, L., Kriz, W., Mundel, P., and D'Agati, V. (1999) *J. Am. Soc. Nephrol.* **10,** 51–61
25. Meyer, G., Varoqueaux, F., Neeb, A., Oschlies, M., and Brose, N. (2004) *Neuropharmacology* **47,** 724–733
26. Wright, G. J., Leslie, J. D., Ariza-McNaughton, L., and Lewis, J. (2004) *Development* **131,** 5659–5669
27. Shih, N. Y., Li, J., Karpitskii, V., Nguyen, A., Dustin, M. L., Kanagawa, O., Miner, J. H., and Shaw, A. S. (1999) *Science* **286,** 312–315
28. Donoviel, D. B., Freed, D. D., Vogel, H., Potter, D. G., Hawkins, E., Barrish, J. P., Mathur, B. N., Turner, C. A., Geske, R., Montgomery, C. A., Starbuck, M., Brandt, M., Gupta, A., Ramirez-Solis, R., Zambrowicz, B. P., and Powell, D. R. (2001) *Mol. Cell. Biol.* **21,** 4829–4836
29. Kos, C. H., Le, T. C., Sinha, S., Henderson, J. M., Kim, S. H., Sugimoto, H., Kalluri, R., Gerszten, R. E., and Pollak, M. R. (2003) *J. Clin. Invest.* **111,**

1683–1690
30. Roselli, S., Heidet, L., Sich, M., Henger, A., Kretzler, M., Gubler, M. C., and Antignac, C. (2004) *Mol. Cell. Biol.* **24,** 550–560
31. Putaala, H., Soininen, R., Kilpeläinen, P., Wartiovaara, J., and Tryggvason, K. (2001) *Hum. Mol. Genet* **10,** 1–8
32. Niranjan, T., Bielesz, B., Gruenwald, A., Ponda, M. P., Kopp, J. B., Thomas, D. B., and Susztak, K. (2008) *Nat. Med.* **14,** 290–298
33. Waters, A. M., Wu, M. Y., Onay, T., Scutaru, J., Liu, J., Lobe, C. G., Quaggin, S. E., and Piscione, T. D. (2008) *J. Am. Soc. Nephrol.* **19,** 1139–1157
34. Henderson, J. M., Al-Waheeb, S., Weins, A., Dandapani, S. V., and Pollak, M. R. (2008) *Kidney Int.* **73,** 741–750
35. Eremina, V., Sood, M., Haigh, J., Nagy, A., Lajoie, G., Ferrara, N., Gerber, H. P., Kikkawa, Y., Miner, J. H., and Quaggin, S. E. (2003) *J. Clin. Invest.* **111,** 707–716
36. Barisoni, L., Madaio, M. P., Eraso, M., Gasser, D. L., and Nelson, P. J. (2005) *J. Am. Soc. Nephrol.* **16,** 2847–2851
37. Kopp, J. B., Klotman, M. E., Adler, S. H., Bruggeman, L. A., Dickie, P., Marinos, N. J., Eckhaus, M., Bryant, J. L., Notkins, A. L., and Klotman, P. E. (1992) *Proc. Natl. Acad. Sci. U.S.A.* **89,** 1577–1581
38. Dobrosotskaya, I. Y., and James, G. L. (2000) *Biochem. Biophys. Res. Commun.* **270,** 903–909
39. Emtage, L., Chang, H., Tiver, R., and Rongo, C. (2009) *PLoS ONE* **4,** e4613
40. Mizuhara, E., Nakatani, T., Minaki, Y., Sakamoto, Y., Ono, Y., and Takai, Y. (2005) *J. Biol. Chem.* **280,** 26499–26507
41. Mundel, P., Reiser, J., Zúñiga Mejía Borja, A., Pavenstädt, H., Davidson, G. R., Kriz, W., and Zeller, R. (1997) *Exp. Cell Res.* **236,** 248–258